 doi:10.20944/preprints202103.0293.v1

Article

The Modulating Effect of Ethanol on the Morphology of a Zr-based Metal-Organic Framework under Room Temperature in the Cosolvent System

Yunzhuo Li[1], Zirong Tang[2], Chen Chen[2,*]

1 Wuhan Britain-China School; liyunzhuotr@gmail.com

2 Huazhong University of Science and Technology;

* Correspondence: chenchen_@hust.edu.cn

Abstract: We report that ethanol, used together with water, plays a crucial role in tuning the structures of a zirconium-based Metal-Organic Framework, the 12-connected MOF-801, and the possible mechanisms of this modulating effect. By employing the cosolvent system of ethanol and water just under room temperature without the presence of a monotopic carboxylic acid as the modulator, MOF-801 in various morphologies of different sizes can be synthesized. The linear correlation between the ethanol/water ratio and the crystal sizes is also demonstrated. The growth mechanism is mainly explained by ethanol's binding with the metal ion clusters and the Marangoni Flow Effect. Ethanol competes with the linker molecules in coordinating with the Zr metal clusters, a role similar to that of the modulators. The Marangoni Flow Effect, which dominates at a certain solvent ratio, further promotes the 1-D alignment of the MOF-801 crystals.

Citation: Li, Y.;Tang, Z.; Chen, C. Ms. *Nanomaterials* **2021**, *11*, x. https://doi.org/10.3390/xxxxx

Keywords: Metal-Organic Framework; MOF-801; Modulators; Ethanol; Marangoni Flow Effect.

1. Introduction

Metal-Organic Frameworks (MOFs), a group of porous crystalline materials, have raised a few eyebrows due to their high surface area[1]. The permanent porosity of the MOFs allows gas molecules to move in and out without barriers, making them a promising material for gas absorption and storage[2-3]. Among all the MOFs that have been synthesized, Zr-based ones have a proper place due to their large family ranging from 6-connected to 12-connected. MOF-801 is a Zr-based MOF that stands out prominently for its considerable water absorption capability under atmospheric pressure and room temperature[4]. It encompasses the 12-connected $Zr_6O_4(OH)_4$ secondary building units (SBUs) and linear ditopic fumaric acid linkers. The low reversibility of Zr-O bonds makes the synthesis of high crystallinity challenging[1]. Zr-based MOFs are commonly synthesized by reacting an appropriate metal source with organic linker molecules dissolved in an organic amide solvent with certain modulator (typically monocarboxylic acids such as formic, acetic, or benzoic acid) at temperatures ranging from 60 to 140 degrees Celsius for several hours or several days[1,5]. The MOFs synthesized without the presence of a

Preprints (www.preprints.org) | NOT PEER-REVIEWED | Posted: 10 March 2021 doi:10.20944/preprints202103.0293.v1

modulator are often amorphous or of poor crystallinity[6]. The modulator molecules bind with the SBUs formed in-situ at certain positions, blocking the extension of the structure in these specific directions, allowing polyhedron MOF crystals with higher crystallinity to form[7]. Schaate et al. have reported that the Zr-based metal-organic frameworks obtained by exclusively mixing the water solution of the metal source and fumaric acid without modulators, however, is amorphous with disappointingly low crystallinity, as the water increases the reticulation rate[8]. By using two solvents, or with say the cosolvent system, researchers may tune the structures of the MOFs. Changing the ratio between ethanol and water in the synthesis, Jang et al. have been able to synthesize ZIF-67 of various shapes and sizes[9]. But the growth of 12-connected MOF-801 is a different story from that of the single atom metal nodes. The formation of highly crystalline Zr-based MOFs is rather challenging, limiting the scale of their mass production. Dai et al. have come up with a method to synthesize Zr-based MOFs, but still requires the addition of monotopic modulators[10]. Marangoni Flow Effect is the convection between liquids up the surface tension gradient[11]. When the solvent of low surface tension evaporates, the one of higher surface tension simultaneously gathers and condenses near the surface, forming a drag force which promotes the one-directional flow from the low surface tension solvent to the high surface tension solvent. The Marangoni Flow Effect is known to be able to direct the one-directional movement of the nanoparticles , regulating the patterns of these particles[11-12]. We hereby report the role of ethanol on the morphology of the MOF-801 whose structures can be tuned under room temperature by using a water-ethanol cosolvent system, as well as the mechanism during the reticulation. Ethanol, just like fumaric acid, may bind with the metal clusters, serving a purpose similar to that of the modulators. The Marangoni Flow Effect also has a significant impact at specific solvent ratios. However, if not this ratio, the nanocrystals are either too small and far apart or interconnect.

2. Materials and Methods

The zirconium sulfate($Zr(SO_4)_2$, AR, 100g) and fumaric acid($C_4H_4O_4$, AR, 250g) are purchased from Shanghai Zhanyun Co. Ltd. Ethanol(C_2H_5OH, AR, 500ml) is purchased from XILONG SCIENTIFIC Co. Ltd. All the materials are used without further purification.

Various morphologies of MOF-801 have been successfully obtained using a cosolvent system by altering the ratio of water and ethanol. 1.78g zirconium sulfate is dissolved in 20ml of water and 0.59g fumaric acid is dissolved in 20ml of ethanol[13]. The 2 solutions are gently mixed using a dropping pipette. The mixture is placed still in room temperature for 30 minutes to allow nucleation, and then stirred for 240 minutes(4 hours). The white powder of MOF-801 is obtained by centrifugal separation. The sample is washed with the blend of 20 ml water and 20 ml ethanol for 3 times and pure ethanol for 2 times. Then it is dried under 60 degrees Celsius for 3 hours.

Then the Ceteris Paribus experiments are carried out. The mass of the zirconium sulfate and the fumaric acid are fixed, while the ratio between ethanol and water are changed to 2, 3, 4, 0.5, 0.33 and 0.25. We first fix the volume of water at 20 ml and change the volume of the ethanol added to 40 ml, 60 ml and 80 ml. Then we fix the volume of ethanol and increase the volume of water added to 40 ml, 60 ml and 80 ml. At last, the rest of the above procedures are repeated every time we change to obtain MOF-801 crystals.

All the samples prepared are then sent for characterization. The SEM tests are carried out on a JEOL JCM-6000 scanning electron microscope. Powder X-Ray Diffraction(PXRD) is performed on a Bruker AXS D8 with copper as the radiation source. The compositions

Preprints (www.preprints.org) | NOT PEER-REVIEWED | Posted: 10 March 2021 doi:10.20944/preprints202103.0293.v1

of the materials are determined by X-Ray Photon Spectroscopy on the Omicron Dar400 with an achromatic aluminium X-ray source. The specific functional groups present in the material are investigated by FT-IR on PerkinElmer Frontier.

3. Results and Discussion

All of the various morphologies of the MOF-801 samples as well as their PXRD patterns are shown in Figure 1. The morphology of MOF-801 crystals formed in 20 ml water and 20 ml ethanol resembles polyhedrons sized approximately 100 nm.

The ratio between ethanol and water is changed to 2. When the ratio of ethanol to water increases, the solution turns turbid more slowly, indicating lower reticulation rate. The samples obtained signify the morphology of rods. When the ratio of water to ethanol comes to 20 ml: 60 ml and 20 ml: 80 ml, relatively large polyhedral granules sized about 300 nm and 500 nm are obtained. The XRD analysis shown in Figure 1 shows the phase-pure synthesis of the MOF-801 crystals.

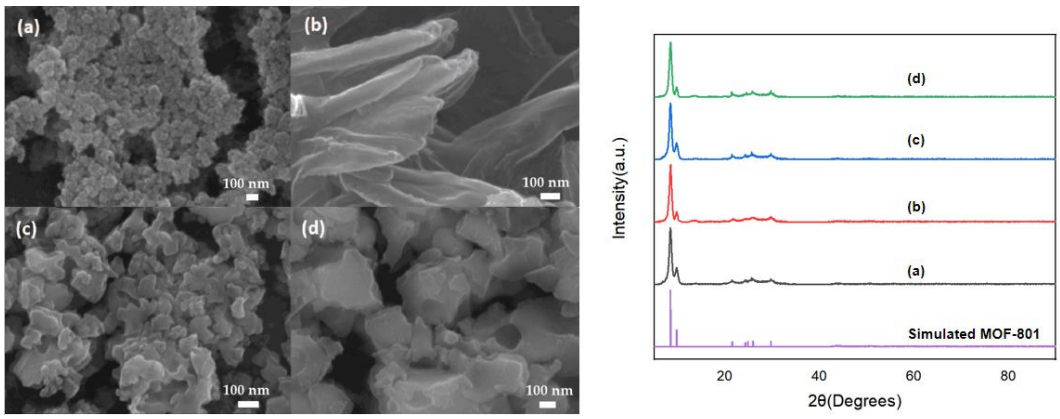

Figure 1. SEM and XRD diagrams of the samples prepared in (a) 20 ml water, 20 ml ethanol, polyhedrons of approximately 100 nm; (b) 20 ml water, 40 ml ethanol, rods; (c) 20 ml water, 60 ml ethanol, polyhedrons of approximately 300 nm; (d) 20 ml water, 80 ml ethanol, large polyhedrons of approximately 500 nm.

Ceteris Paribus, the ratio of ethanol to water is then decreased below 1. When the proportion of water in the reaction increases, the white precipitate forms much faster, indicating a higher rate of nucleation. When the volume of water is 40 ml, the polyhedron granules sized approximately 40 nm are obtained. These granules begin to show partial interconnection, with a small minority of the crystals accreting. Then, when the volume of water comes to 60 ml and 80 ml, the small nanosized polyhedrons of lengths less than 10 nm that are intergrown and cannot be separated by ultrasound are observed, as shown in Figure 2. It is noted in the XRD diagrams in both Figure 1 and Figure 2 that as the ratio between ethanol and water decreases, the peaks become lower and wider, indicating smaller crystal sizes of the MOF-801 crystals. This is coherent with our observations from the SEM that decreasing the ratio leads to the fall in crystal size.

Preprints (www.preprints.org) | NOT PEER-REVIEWED | Posted: 10 March 2021 doi:10.20944/preprints202103.0293.v1

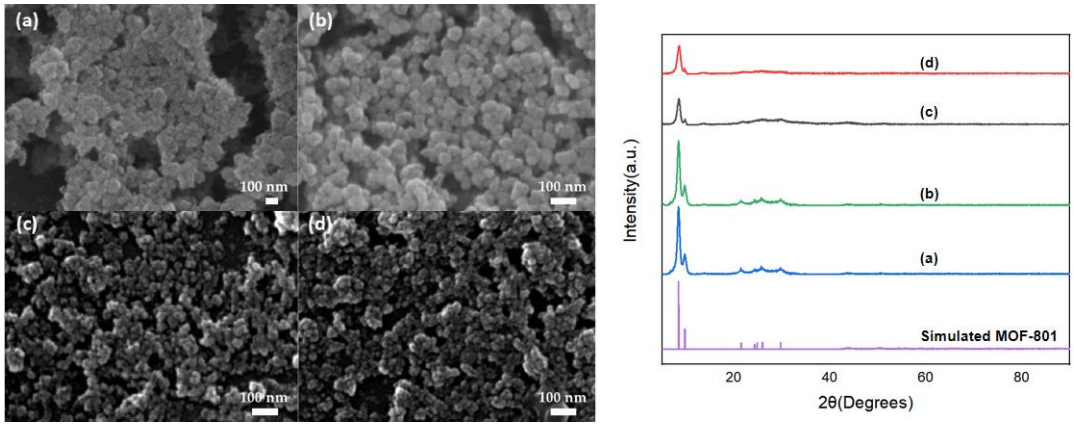

Figure 2. SEM and XRD diagrams of the samples prepared in (a) 20 ml water, 20 ml ethanol, polyhedrons of approximately 100 nm; (b) 40 ml water, 20 ml ethanol, granules of approximately 40 nm; (c) 60 ml water, 20 ml ethanol, intergrown nanosized crystallites; (d) 80 ml water, 20 ml ethanol, intergrown nanosized crystallites.

We notice the exception of the shape of the MOF-801 when the solvent ratio is 2. In order to understand the process of the growth of this kind of rod-like MOF crystals, we perform the ex-situ analysis during the growth of the MOF-801 nanorods[9]. As shown in Figure 3, we are able to determine the phases that the MOF-801 crystals undergo in the reticulation process. We obtain the samples under different reaction times i.e. 15 seconds, 30 minutes and 3 hours. When we analyze the MOF-801 samples formed in 20 ml water and 40 ml ethanol in 15 seconds, we may observe the one-directional alignment of the thread-like crystals that are interconnected. Though the crystals are not separated from each other, the preferred growth direction of these crystals is identical. When the reticulation time comes to 30 minutes, the one-directional alignment of the crystal growth can still be observed. The crystals grow towards the identical direction, but each single crystallite begins to separate from each other. The interconnected structures begin to collapse and the single crystals start to form. When the reaction proceeds to 4 hours, the rod-shaped MOF-801 single crystals become independent from each other.

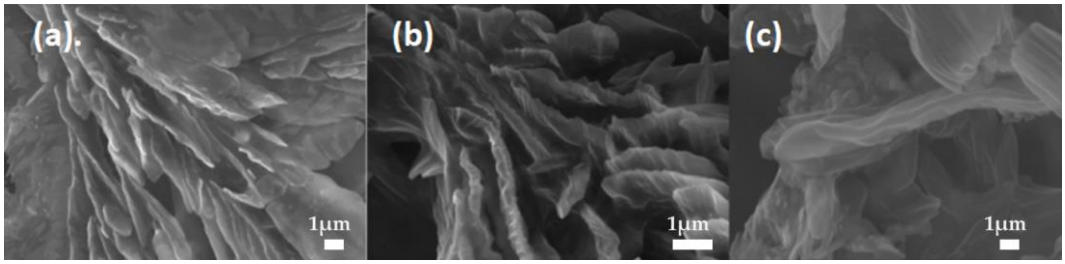

Figure 3. The ex-situ analysis after the reticulation starts for:(a)15 seconds;(b)30 minutes;(c)3 hours.

With the aim of determining the relationship between the volume ratio of ethanol to water and the crystal sizes, we use EXCEL to plot a best-fit line by linear fitting. The linear fitting graph is shown in Figure 4 that follows. The trend of the crystal size changing with the ratio seems to be linear.

We then calculate the Pearson Correlation Coefficient between the 2 variables. The Pearson Correlation Coefficient is a measure of the the linear relation between variables. The closer it is to 1 or -1, the more 'linear' the relationship is. The correlation coefficient can be derived from the following equation:

Preprints (www.preprints.org) | NOT PEER-REVIEWED | Posted: 10 March 2021 doi:10.20944/preprints202103.0293.v1

$$\rho_{X,Y} = \frac{N\sum XY - \sum X \sum Y}{\sqrt{N\sum X^2 - (\sum X)^2}\sqrt{N\sum Y^2 - (\sum Y)^2}} \quad \text{(a)}$$

The Pearson Correlation Coefficient between crystal sizes and the volume ratio is +0.991184862, which is far more than +0.8 and the correlation is considered strongly linear. We then use linear-fitting via Excel to further demonstrate this linear relationship. The errors when reading the lengths of the crystals is considered 50 nm. The linear relationship can best be demonstrated in the best-fit line in Figure 4 below. The gradient of the line is 124.05, which means a increase in size of 124.05 nm every time the ratio increases by 1 and greater or equal to 0.25. The MATLAB code can be found in the Appendix 1.

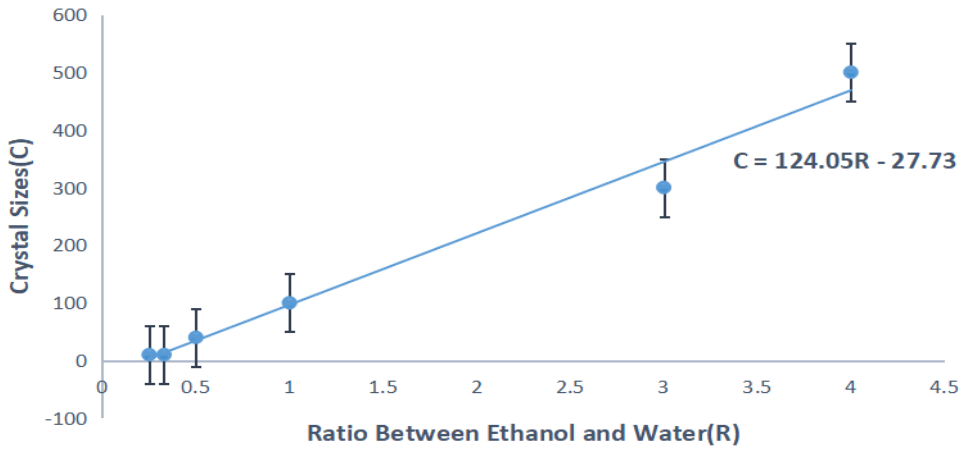

Figure 4. The linear relationship between the volume ratio of ethanol to water and crystal size.

Water is known to have the ability to foster the formation Zr-based metal-organic frameworks. In 2011, Schaate et al. reported that water can increase the rate of the formation of UiO-66, a Zr-based MOF with 12-connected SBUs, straight ditopic linkers and fcu topology similar to MOF-801. The OH^- ions in water is a key component in the $Zr_6O_4(OH)_4$ SBUs of the 12-connected Zr-based MOF, which consists of both O^{2-} and OH^- ions. With increasing water content, the solution turned turbid more quickly, which indicated a higher aggregation rate. The increase in the rate of formation of the crystallites signifies lower possibility for error correction, leading to intergrown structures with low crystallinity. Ethanol, on the other hand, decreases the rate of the solution turning turbid. The relatively low aggregation rate caused by the increased ratio of ethanol to water is responsible for the bigger single crystals of higher crystallinity. But what causes the aggregation rate to decrease when the ratio of ethanol to water declines?

To further investigate the role of ethanol in the formation of MOF-801, we apply infrared spectrometry to investigate the specific bonds and functional groups present in the SBU[14]. The black line in Figure 5 demonstrates the infrared spectra of MOF-801 formed in 20 ml ethanol and 80 ml water, named Sample (a), while the red line for that synthesized in 80 ml ethanol and 20 ml water, named sample (b).

Preprints (www.preprints.org) | NOT PEER-REVIEWED | Posted: 10 March 2021 doi:10.20944/preprints202103.0293.v1

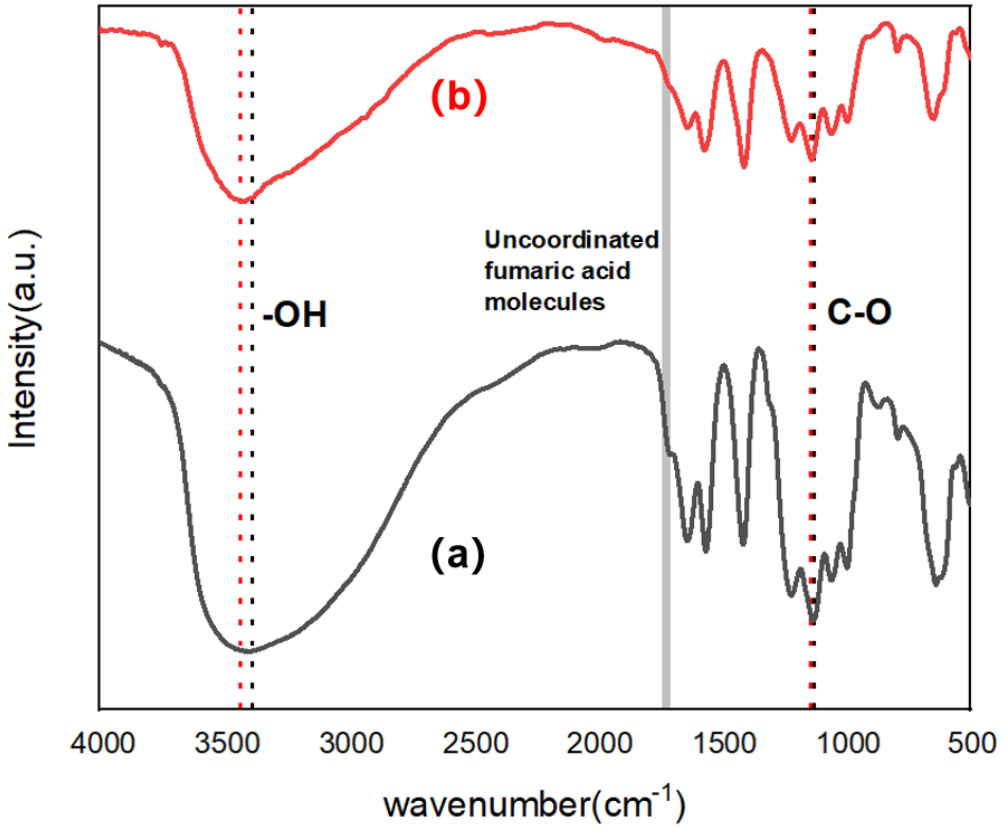

Figure 5. The infrared spectra of MOF-801 formed in: (a) 80 ml ethanol, 20 ml water; (b) 20 ml ethanol, 80 ml water.

The wavenumbers of some of their stretching vibration peaks are shown in Table 1. From the infrared spectra in Figure 5 and the wavenumbers of the peaks in Table 1, we inspect that the growth mechanism of the MOF-801 of different morphologies can mainly be explained by ethanol's binding with the Zr metal clusters. We hereby suspect that the ethanol molecules may form coordination bonds with the zirconium ions, blocking the extension of the structure in this specific direction. This is just like modulating the formation of MOF-801 crystals. Ordinary carboxyl groups, due to the carbonyl groups, exhibit peaks at around 1720 cm^{-1}. If no dimers formed, they also show peaks over 3550 cm^{-1} corresponding to the hydroxyl groups, or numerous consecutive small peaks between 2500 cm^{-1} and 3500 cm^{-1}, in carboxylic acid dimers. Nevertheless, neither of the IR patterns of these 2 samples show peaks around 3550 cm^{-1} or 1720 cm^{-1}. They also lack any consecutive peaks between 2500 cm^{-1} and 3500 cm^{-1}. Instead, they have peaks at around 1400 cm^{-1} and 1550 cm^{-1}, which signifies the absence of the -COOH group, or with say the absence of uncoordinated fumaric acid linker molecules, and the exclusive presence of COO^{-}[10]. The 1400 cm^{-1} peak represents the symmetric stretch vibration of COO^{-}, while the 1550cm^{-1} peak is the asymmetric stretch vibration for it. According to Dai et al., the IR pattern of the common MOF-801 does not exhibit any strong peaks at around 3400 cm^{-1}[10]. But there are exceptionally strong absorption peaks in these 2 samples at around 3400 cm^{-1}.

Table 1. The absorption peaks of the MOF-801 formed in: (a) 80 ml ethanol, 20 ml water;(b) 20 ml ethanol, 80 ml water.

Preprints (www.preprints.org) | NOT PEER-REVIEWED | Posted: 10 March 2021 doi:10.20944/preprints202103.0293.v1

Samples / Stretching vibrations / Bonds	(a)	(b)
OH-	3388.46 cm^{-1}	3429.72 cm^{-1}
COO^-	1412.3 cm^{-1}	1409.09 cm^{-1}
C-OH	1130.72 cm^{-1}	1137.37 cm^{-1}

These strong peaks might be caused by the hydroxyl groups of ethanol molecules that bind with the metal nodes[15-16]. The peak for the stretching vibration of the hydroxyl group in ethanol, on the other hand, is at about 3318 cm^{-1}. The samples obtained after the reaction in 20 ml ethanol and 80 ml water exhibits a peak at 3388 cm^{-1}, 78 cm^{-1} higher than the hydroxyl group in ethanol. Similarly, the samples obtained in 80 ml ethanol and 20 ml water, similarly, exhibits a peak at 3429 cm^{-1}, 111 cm^{-1} higher than that of the normal hydroxyl group in ethanol. This is because when ethanol binds with the Zr(IV) ions, the empty d-orbitals of the zirconium ions withdraw electrons from the oxygen atoms of ethanol that are rich in electrons, causing a blue shift of the absorption peaks for the hydroxyl groups. This blue shift explains the higher wavelengths absorbed by the hydroxyl groups. The higher the proportion of ethanol, the more ethanol coordinates with the metal ions, the higher the wavenumber is.

The ethanol's binding with the metal ions, also, may explain the blue shift of the peak of the C-O bond. The peak for the stretching vibration of C-O bond in ethanol is at 1038 cm^{-1}. When it comes to the as-synthesized sample, the peak shifts to around 1130 cm^{-1}.and the intensity of the peak decrease. Due to the electron-withdrawing effect of the Zr ions, the blue-shift of the peak occurs due to an increase in chemical shift[10]. Furthermore, when the proportion of ethanol increases, the intensities for the peaks corresponding to the C-O bonds and the -OH groups decreases significantly, which is shown in Figure 7. This decrease in intensity may further prove that ethanol coordinates with the metal ions, causing a redistribution of the electrons on the hydroxyl group[17].

We then carry out the XPS narrow scan analysis to investigate the element content on the surface of the MOF-801 samples. The ratio of oxygen and carbon inside the samples prepared in (a) 80 ml ethanol, 20 ml water; (b) 20 ml ethanol, 80 ml water are shown in Figure 6 below. The percentages of the elements in the samples are shown in Table 2.

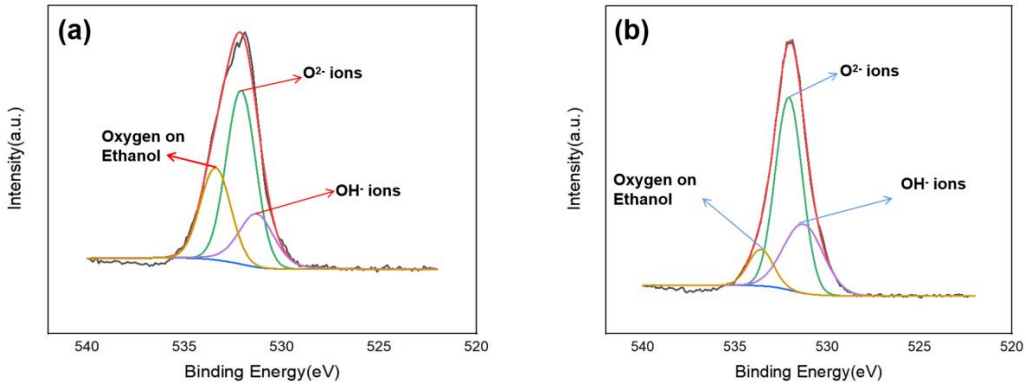

Preprints (www.preprints.org) | NOT PEER-REVIEWED | Posted: 10 March 2021 doi:10.20944/preprints202103.0293.v1

Figure 6. The XPS narrow scan analysis of the oxygen atoms in the MOF-801 samples prepared in (a) 80 ml ethanol, 20 ml water; (b) 20 ml ethanol, 80 ml water.

One thing we find interesting is that there are 3 peaks for the 1s orbital of oxygen at around 530.4 eV, 531.9 eV and 533.8 eV, which signifies the 3 environments for oxygen atoms. Amongst these 3 peaks, the one at 531.9 eV represents the O^{2-} and the 530.4 eV one is the OH^- ions incorporated in the SBUs of the MOF-801, which is fairly close to the previously reported values[18]. So why is there still another peak at 533.8 eV?

We have concluded from Figure 5 that there aren't any unbounded fumaric acid molecules, so the only possibility for the other peak is the oxygen atom on ethanol which coordinates with zirconium. We may conclude that the shift in the peak for the hydroxyl group is caused by ethanol molecules' binding with the metal clusters. During the reticulation process when the metal ions cluster together to form stable SBUs, the ethanol molecules also bind with the ions of zirconium due to the strong 'oxophilicity' of zirconium ions. In this way, the structural defects emerge on the metal nodes due to missing linker. Because zirconium ions have empty orbitals and may thus withdraw electrons from the hydroxyl groups of the ethanol molecules, the blue shift of the hydroxyl group is observed. For the strength of the Zr-O bonds, the ethanol molecules are not removed in the evacuation step, which washes away the guest molecules residing inside the pores.

Another thing that intrigues us is the different percentage ratio of the oxygen and carbon elements. Table 2 further demonstrates that, the higher the ratio of ethanol, the larger the proportion of carbon, and the smaller proportion of oxygen in the as-synthesized sample. The sample synthesized in 20 ml water and 80 ml ethanol has 49.01% of carbon and only 33.49% of oxygen by mass, while that synthesized in 80 ml water and 20 ml ethanol contains smaller proportion of carbon of 33.49% and higher proportion of oxygen of 45.11%. That is to say that more ethanol leads to more carbon atoms and relatively less oxygen atoms in the coordination network of MOF-801, which is coherent with our suggestion that ethanol binds with the metal nodes.

Table 2. The percentage ratio of the oxygen and carbon in the samples.

Samples / Percent Ratio / Elements	(a)	(b)
O	33.49%	45.11%
C	49.01%	20.32%

Though the function ethanol serves is similar to that of the monotopic modulators, the way in which the ethanol molecules bind with the metal ion clusters is rather different. The differences in their means of binding are illustrated in Figure 7. As shown in Figure 7, the fumaric acid molecules bind with the metal ion clusters in syn-syn bridging mode, in which 2 oxygen atoms on a carboxyl group bind with different Zr ions. This is due to the delocalized Π bond formed in each of the carbonyl groups, which makes the 2 oxygen atoms identical and renders the covalent characteristics of the Zr-O bonds. This strategy is called the syn-syn bridging[1]. This syn-syn bridging strategy explains why the peaks for the linker molecules is around 1400cm-1 and 1550cm-1 rather than 1700cm-1: the 2 C-O bonds are 'average'. While the one topic of the a fumaric acid molecule is connected to 2 zirconium ions, 2 ethanol molecules take the place of this fumaric

Preprints (www.preprints.org) | NOT PEER-REVIEWED | Posted: 10 March 2021 doi:10.20944/preprints202103.0293.v1

acid molecule, each binding with a single zirconium ion. This also constitute a structure similar to syn-syn bridging. The binding of these 2 ethanol molecules will block the extension of the coordination framework in this specific direction.

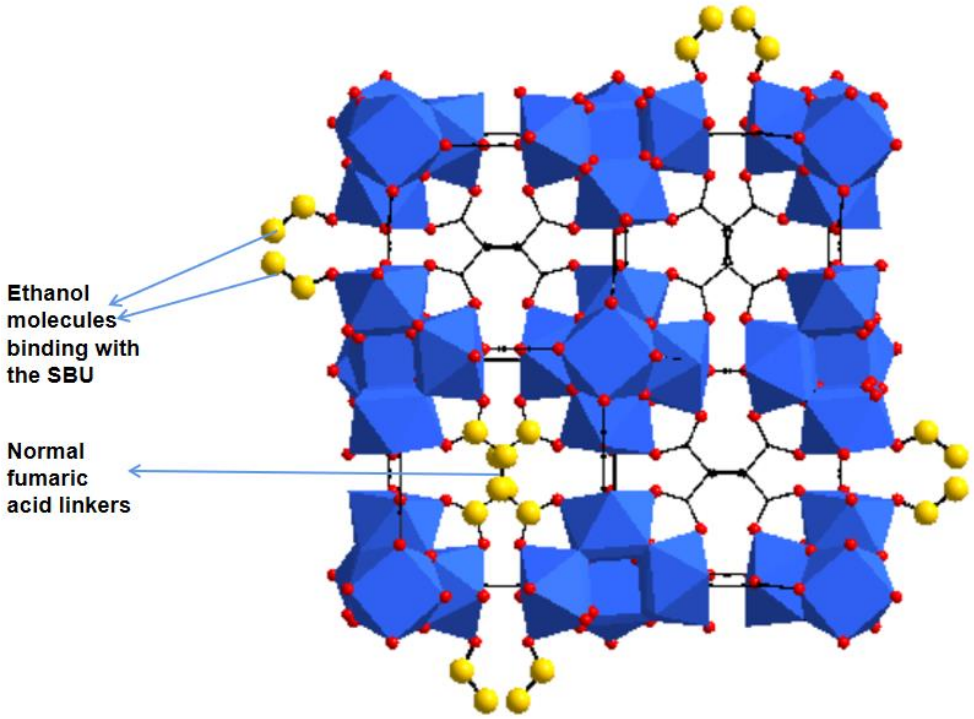

Figure 7. The different binding modes between Zr ions and the organic molecules. All the hydrogen atoms are omitted. The yellow spheres representing carbon atoms are just for clarification purposes.

What, then, may explain the exception of the MOF-801 nanorods samples? Maybe it's the Marangoni Flow Effect. The Marangoni Flow Effect is caused by the surface tension gradient between liquid phases[21]. Cai et al have reported that, when a wet nitrogen gas stream passes the surface of a thin layer of ethanol, as the ethanol phase evaporates, water simultaneously condenses near the contact line[12].

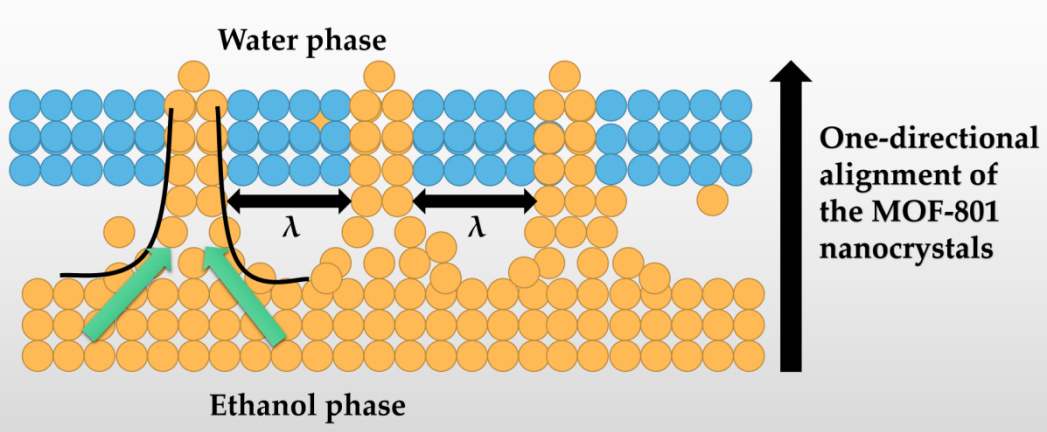

Figure 8. Schematic illustration of the Marangoni Flow between ethanol and water phase.

Here, as shown in Figure 8, when ethanol evaporates, water molecules begin to gather. Because water evaporates slower than ethanol, the condensed water molecules form a

Preprints (www.preprints.org) | NOT PEER-REVIEWED | Posted: 10 March 2021 doi:10.20944/preprints202103.0293.v1

thin water film. Thus, a strong surface tension gradient is generated at the transition zone between the receding ethanol phase and the water phase within a narrow region. The surface tension gradient drives the ethanol, as well as the fumaric acid linker molecules into the water phase. The one-directon flow, therefore, is formed at the interface. When the water is added into ethanol, the large difference in surface tension of the liquids immediately drives the flow of ethanol into water. Then, as the reaction proceeds, ethanol constantly evaporates and condenses, leading to continuous flow of ethanol. This Marangoni Flow directs the 1-d alignment of the coordination network. The characteristic wavelength shown in Figure 8 can be estimated from the following equation (b)[11].

$$\lambda = \frac{2\pi h}{\sqrt{\frac{M_a}{8}}} \tag{b}$$

Where h can be calculated from the average diameter of the water droplets(D) and the contact angle between water droplets and ethanol(θ), as equation (c) shows:

$$h = \frac{D}{2\sin\theta}(1-\cos\theta)$$

Ma is the Marangoni Number that can be derived from the following equation (d):

$$Ma = \frac{\Delta\gamma\Delta T h}{\rho\nu\kappa} \tag{c}$$

$\Delta\gamma$ is the difference in surface tension between solvents; ΔT is the temperature change during reaction; $\rho\nu\kappa$ is a constant for water, approximately 1.45933×10^{-8}[12]. D is 1.1×10^{-4} m, given that a single droplet of water is around 0.05 ml. The difference in surface tension between ethanol (22 mN/m) and water (72 mN/m) is 50 nM/m. In this way, the value of λ is around 0.764 μm. This is different from the value observed in Figure 3, which is over 1 μm. Why this difference?

Maillard et al has reported that this formula could only be used for quantitative estimations[11]. The difference in surface tension could be less than 50 mN/m due to impurities. There is also thermal energy transfer to the surrounding, which may increase the value of temperature change measured. In this way, the characteristic wavelength of the Marangoni Flow could be more than 0.764 μm.

But what about the Marangoni Flow for other solvent ratios? There's still Marangoni Flow, but it does not dominate any longer. When the ratio of ethanol to water reaches 3, the temperature change drops to 0.8 Degrees Celsius. This causes the characteristic wavelength to become larger. The MOF-801 single crystals formed in this way are much larger due to larger distances between each 2 streams of the Marangoni convection. On the other hand, when the ratio becomes 1, the temperature change rises to 7.6 Degrees Celsius. Thus, λ is much smaller, resulting in relatively smaller sizes of the MOF-801 crystals. These nanosized MOF-801 crystals also easily interconnect because of the smaller distances between each 2 streams of convection. In both of these cases, the role that the Marangoni Flow plays does not dominate anymore.

At this point, we want this work to help further researches gain insight into the role that ethanol plays in the synthesis of the MOFs. Future research may further investigate the mechanism of how ethanol modulates the reticulation of all sorts of MOFs or focus on new synthesis strategies of MOFs using ethanol.

 doi:10.20944/preprints202103.0293.v1

4. Conclusion

This work present that ethanol may serve as modulators in the synthesis of MOF-801 under room temperature by its competitive coordination to the SBUs with fumaric acid linker molecules. The work also report the effect of the Marangoni Flow at certain solvent ratio on the morphology of the MOF-801, leading to rod-shaped MOF-801. In this way, different sizes and morphologies of the MOF-801 can be obtained by just changing the solvent ratio of ethanol to water in room temperature. We hope that this work will be promising for the new room-temperature synthesis strategies of Zr-based MOFs and their applications.

Author Contributions: Conceptualization, Yunzhuo Li and Chen Chen; Methodology, Zirong Tang; Project administration, Zirong Tang; Software, Yunzhuo Li and Chen Chen; Supervision, Chen Chen; Validation, Yunzhuo Li; Writing – original draft, Yunzhuo Li; Writing – review & editing, Yunzhuo Li, Zirong Tang and Chen Chen.

Funding: This research received no external funding.

Data Availability Statement: Please refer to the structure of the MOF-801 at https://www.ccdc.cam.ac.uk/.

Acknowledgments: We would like to faithfully thank Prof. Tielin Shi for providing the equipment and raw-materials. We also feel grateful to Suzhou Institute of Nano-Tech and Nano-Bionics which took the XPS, XRD and BET measurements.

Conflicts of Interest: The authors declare no conflict of interest.

Appendix A

```
x=[0.25, 0.33, 0.5, 1, 3, 4]

y=[10, 10, 40, 100, 300, 500]

r1=(x,y,'type','Pearson')

r2=corrcoef(x,y)
```

References

[1]Yaghi, O. M. , Kalmutzki, M. J. , & Diercks, C. S. . (2019). *Introduction to Reticular Chemistry*.

[2]Rostami, M. , Mofarahi, M. , Karimzadeh, R. , & Abedi, D. . (2016). Preparation and characterization of activated carbon–zeolite composite for gas adsorption separation of co2/n2 system. *Journal of Chemical & Engineering Data*.

[3]Putkham, A. . (2010). *Synthesis, characterisation and gas absorption studies for metal organic framework materials*. (Doctoral dissertation).

[4]Furukawa, H. , Gandara, F. , Zhang, Y. B. , Jiang, J. , Queen, W. L. , & Hudson, M. R. , et al. (2014). Water adsorption in porous metal-organic frameworks and related materials. *Journal of the American Chemical Society, 136*(11), 4369.

[5]Li, H. L. , Eddaoudi, M. M. , O'Keeffe, M. , & Yaghi, O. M. . (1999). Design and synthesis of an exceptionally stable and highly porous metal-organic framework. *Nature, 402*(6759).

[6]Ren, J. , Langmi, H. W. , North, B. C. , Mathe, M. , & Bessarabov, D. . (2014). Modulated synthesis of zirconium-metal organic framework (zr-mof) for hydrogen storage applications. *International Journal of Hydrogen Energy, 39*(2), 890–895.

[7]WilMann, G. , Schaate, A. , Lilienthal, S. , Bremer, I. , Schneider, A. M. , & Behrens, P. . (2012). Modulated synthesis of Zr-fumarate MOF. *Microporous and Mesoporous Materials, 152*(none), 64–70.

[8]Andreas, Schaate, Pascal, Roy, Prof. Dr., & Adelheid, et al. (2011). Modulated synthesis of zr-based metal–organic frameworks: from nano to single crystals. *Chemistry - A European Journal*.

[9]Ji-Soo, Jang, Won-Tae, Koo, Dong-Ha, & Kim, et al. (2018). In situ coupling of multidimensional mofs for heterogeneous metal-oxide architectures: toward sensitive chemiresistors. *ACS central science*.

[10]Dai, S. , Nouar, F. , Zhang, S. , Tissot, A. , & Serre, C. . (2020). One-step versatile room temperature synthesis of metal(iv) carboxylate mofs. *Angewandte Chemie*.

[11]Maillard, M. , Motte, L. , & M.cc. Pileni. (2001). Rings and hexagons made of nanocrystals. *Advanced Materials, 13*(3), 200-204.

[12]Cai, Y. , & Newby, B. M. Z. . (2008). Marangoni flow-induced self-assembly of hexagonal and stripelike nanoparticle patterns. *Journal of the American Chemical Society, 130*(19), 6076-7.

[13]Butova, V. V. , Pankin, I. A. , Burachevskaya, O. A. , Vetlitsyna-Novikova, K. S. , & Soldatov, A. V. . (2020). New fast synthesis of mof-801 for water and hydrogen storage: modulator effect and recycling options. *Inorganica Chimica Acta, 514*.

[14]Vanasse, G. A. . (1968). Infrared spectrometry. *Analytical Chemistry, 40*(5), 246R+.

[15]Gallignani, M. , Garrigues, S. , & Miguel, D. L. G. . (1993). Direct determination of ethanol in all types of alcoholic beverages by near-infrared derivative spectrometry. *Analyst, 118*(9), 1167-1173.

[16]Yamaguchi, T. , Nakano, Y. , & Tanabe, K. . (1978). Infrared study of surface hydroxyl groups on zirconium oxide. *Bulletin of the Chemical Society of Japan, 51*(9), 2482-2487.

[17]Song, X., Xiong, J., Shen, X., Lan, Y.. (2016). Study on the Interaction between Zirconium Sulfate with Ethanol, PEG-200 or Ethylene Glycol. *Process and Technology.*

[18]Jin, Z. , Huijuan, B. , Qiu, R. , Hong-Bin, L. , Xiaoming, R. , & Zheng-Fang, T. , et al. (2018). Extra water- and acid-stable mof-801 with high proton conductivity and its composite membrane for proton-exchange membrane. *ACS Applied Materials & Interfaces, 10*, acsami.8b09070-.

[19]Majewski, M. B. , Noh, H. , Islamoglu, T. , & Farha, O. K. . (2018). Nanomofs: little crystallites for substantial applications. *Journal of Materials Chemistry A*, 10.1039.C8TA02132E.

[20]Choi, Jongwon, Lin, Li-Chiang, Grossman, & Jeffrey, et al. (2018). Role of structural defects in the water adsorption properties of mof-801. *Journal of Physical Chemistry C Nanomaterials & Interfaces*.

[21]Xu, X. , & Luo, J. . (2007). Marangoni flow in an evaporating water droplet. *Applied Physics Letters, 91*(12), 3972.

[22]Leeuwen, P. W. N. M. V. . (1967). Alcohols as ligands. i. crystalline hexa-ethanol metal salts. , *86*(3), 247-253.

[23]Tilset, M. , Larabi, C. , Quadrelli, E. A. , Bonino, F. , Lillerud, K. P. , & Kandiah, M. , et al. (2010). Synthesis and stability of tagged uio-66 zr-mofs. *Chemistry of Materials, 22*(24), 6632-6640.

[24]Jasuja, H. , Zang, J. , Sholl, D. S. , & Walton, K. S. . (2016). Rational tuning of water vapor and co2 adsorption in highly stable zr-based mofs. *Journal of Physical Chemistry C, 116*(44), 23526–23532.

[25]Bon, V. , Senkovska, I. , Weiss, M. S. , & Kaskel, S. . (2013). Tailoring of network dimensionality and porosity adjustment in zr- and hf-based mofs. *Crystengcomm, 15*(45), 9572-9577.

[26]A, Q. Y. , A, D. Z. , B, L. V. H. , A, F. Y. , A, T. X. , & B, E. J. M. H. , et al. (2015). Selective liquid phase hydrogenation of furfural to furfuryl alcohol by ru/zr-mofs. *Journal of Molecular Catalysis A: Chemical, 406*(11), 58-64.

[27]Hozawa, M. , Inoue, M. , Sato, J. , Tsukada, T. , & Imaishi, N. . (2006). Marangoni convection during steam absorption into aqueous libr solution with surfactant. *Journal of Chemical Engineering of Japan, 24*(2), 209-214.

[28]Bergeon, A. , Henry, D. , Benhadid, H. , & Tuckerman, L. S. . (2007). Marangoni convection in binary mixtures with soret effect. *Journal of Fluid Mechanics, 375*, 143-177.

[29]Jin, Z. , Huijuan, B. , Qiu, R. , Hong-Bin, L. , Xiaoming, R. , & Zheng-Fang, T. , et al. (2018). Extra water- and acid-stable mof-801 with high proton conductivity and its composite membrane for proton-exchange membrane. *ACS Applied Materials & Interfaces, 10*, acsami.8b09070-.

[30]Ameloot, R. , Vermoortele, F. , Vanhove, W. , Roeffaers, M. , Sels, B. , & De Vos, D. . (2011). Interfacial synthesis of hollow mof capsules demonstrating selective permeability. *Nature Chemistry, 3*(5), 382-387.

[31]Hulsenbeck, L. , Luo, H. , Verma, P. , Dane, J. , Ho, R. , & Beyer, E. , et al. (2020). A Generalized Approach for Rapid Aqueous MOF Synthesis by Controlling Solution pH. *Cryst. Growth Des,* 20(10), 6787–6795